Organic Thin-Film Memory

Yang Yang, Liping Ma, and Jianhua Wu

Abstract

Recently, organic nonvolatile memory devices have attracted considerable attention due to their low cost and high performance. This article reviews recent developments in organic nonvolatile memory and describes in detail an organic electrical bistable device (OBD) that has potential for applications. The OBD consists of a tri-layer of organics/metal nanoclusters/organics sandwiched between top and bottom electrodes. A sufficiently high applied bias causes the metal nanoparticle layer to become polarized, resulting in charge storage near the two metal/organic interfaces. This stored charge lowers the resistance of the device and leads to an electrical switching behavior. The ON and OFF states of an OBD differ in their conductivity by several orders of magnitude and show remarkable bistability—once either state is reached, the device tends to remain in that state for a prolonged period of time. More important, the conductivity states of an OBD can be precisely controlled by the application of a positive voltage pulse (to write) or a negative voltage pulse (to erase). Device performance tests show that the OBD is a promising candidate for high-density, low-cost electrically addressable data storage applications.

Keywords: *nonvolatile memory, OBD, organic electrical bistable devices, rewritable memory, thin films.*

Brief Review of Recent Works on Organic Memory

Organic memory devices are generally realized by interposing thin layers containing organic materials between two electrodes. One way to achieve this is by using an *x*–*y* addressable array format. The array is formed by the cross-points between the parallel bottom electrodes in the *x* direction and the parallel top electrodes in the *y* direction.[1] This format may soon be realized in practical applications, but the data storage density it provides is limited by the cross-point area. Another method involves using probing heads to replace the top electrodes, where the active medium is deposited on top of a conducting substrate, which is used as the common electrode. Generally, scanning probe microscope (SPM) techniques are used for this kind of nanometer-scale memory,[2] with the main advantage of using this technique being ultrahigh data storage density. One of the major drawbacks is that this technique holds little promise from a practical application point of view. In this article, we focus on *x*–*y* addressable organic memories.

The advantages of organic memory devices include, but are not limited to, flexibility, easy processing, low cost, and larger-area fabrication by printing techniques. Another promising possibility is to stack several memory layers on top of each other to enhance the data storage density. Ferroelectric switching and conductance switching have been observed in organic memories. Ferroelectric polymers have a much lower permittivity and switching speed than inorganic ferroelectrics,[3] which makes them less attractive. On the other hand, significant research has been done on resistance switching, dating back to the 1970s. Initially, the focus was on organic thin-film memory in a charge transfer complex system, as proposed by Potember et al.,[4] where the transition between the high-conductance and low-conductance states is realized by charge transfer between copper and tetracyanoquinodimethane (TCNQ). Switching was also observed in polymer films.[5–8] Unfortunately, most of the earlier observed electrical memory effects turned out to be due to filament formation, and the performance was not satisfactory for practical applications. Recently, the search for new types of organic memory began for the purpose of addressing real-world applications. Adachi et al. demonstrated a switching effect in Cu:TCNQ charge transfer complex thin films, where a thin Al_2O_3 layer between the anode and the Cu:TCNQ layer is critical to the observed switching phenomenon.[9] Writing and erasing was realized by applying positive and negative electric fields ($\sim 10^6$ V/cm), respectively, to the films. The ON/OFF ratio can reach as high as 10^4. No mention of write–erase cycle tests or retention tests were found in this report.

Pal et al. reported that conductance switching between three levels can be achieved in supramolecular structures of rose bengal ($C_{20}H_2Cl_4I_4Na_2O_5$),[10] where electroreduction and conformational change of the molecules cause conjugation modification, and as a result, the conductance of the molecules is changed. The ON/OFF ratio can go to 10^5. There is no report about the switching speed in such systems, but one can imagine that if the switching is caused by molecular conformation change under applied electric field, the switching time should be on the nanosecond scale. More work needs to be done in order to clarify the actual device operation mechanism.

Forrest et al. demonstrated a write-once/read-many-times memory by burning polymer fuses,[11,12] where a thin conducting polymer layer, or fuse, made of poly(3,4-ethylenedioxythiophene) (PEDOT) is sandwiched between two electrodes. The as-deposited device shows high conductance due to the conducting polymer PEDOT, but when a burning-voltage pulse is applied (a write process), the polymer fuses will burn and cause the device to be in open-circuit condition (low-conductance state). The write process can be as short as microseconds, depending on the thickness of the PEDOT layer and the amplitude of the applied voltage pulse.

Recently, a research group at UCLA demonstrated several approaches to memory devices. One such approach involves controlling copper ions within the organic layer.[13] The device structure is copper anode/buffer layer/organic layer/cathode. The switching-on process is realized by applying a positive voltage pulse between the two electrodes, driving Cu^+ ions into the organic layer to transform the device into the high-conductance state. An interesting aspect is that a relatively high voltage pulse can drive the Cu^+ ions out of the organic layer and restore the device to the low-conductance state. The beauty of the device is that the switching-on voltage can

be as low as 0.2 V, the ON/OFF ratio can be as high as 10^8, and the retention time of both ON state and OFF state is more than six months. This device is ideal for flash memory applications.

The other memory device proposed by the UCLA group is the organic electrical bistable device (OBD), an organic/metal nanoclusters/organic tri-layer structure sandwiched between two electrodes[14–19] that shows nonvolatile memory behavior. The high-conductance state (ON state) and the low-conductance state (OFF state) differ in their conductance by as much as 10^6 times and show a remarkable retention time. Organic memory devices based on the organic/metal nanoclusters/organic structure have also been reported by other groups.[20,21] Details on OBD studies are discussed later in this article.

Functional organic molecules may also show electrical bistable behavior and have been tested in cross-point memory structures.[22–25] A sandwiched organic film can be fabricated by means of Langmuir–Blodgett (LB) film technology or self-assembled monolayers (SAMs). Two kinds of molecular memories have been reported. One uses a bistable molecule that has two conformers (conformations); the two conformers convert when driven by applying a voltage. Stoddart and Heath et al. reported an electrical bistable device using bistable catenane as the active material.[22,23] The active layer is prepared by LB film technology.

The molecular structure of the catenane and the device working principle are shown in Figure 1.[22] Catenane (Figure 1a) consists of a tetracationic cyclophane that incorporates two bipyridinium units, interlocked with a crown ether containing a tetrathiafulvalene (TTF) unit and a 1,5-dioxynaphthalene (NP) ring system located on opposite sides of the crown ether. The switching mechanism is illustrated in Figure 1b. The ground state "co-conformer" [A^0] of this catenane has the TTF unit located inside the cyclophane. Upon oxidation, the TTF unit becomes positively charged, and the Coulombic repulsion between TTF^+ and the tetracationic cyclophane causes the crown ether to circumrotate to give co-conformer [B^+], which will reduce back to [B^0] when the bias is returned to 0 V. This bistability is the basis of this device. The energy gap between the highest occupied and lowest unoccupied molecular orbitals for co-conformer [B^0] must be narrower in energy than the corresponding gap in co-conformer [A^0], implying that, in a solid-state device, tunneling current through the junction containing [B^0] will be greater. Thus, this co-conformer represents the "closed switch" state, and the ground state co-conformer [A^0] represents the "open switch" state.

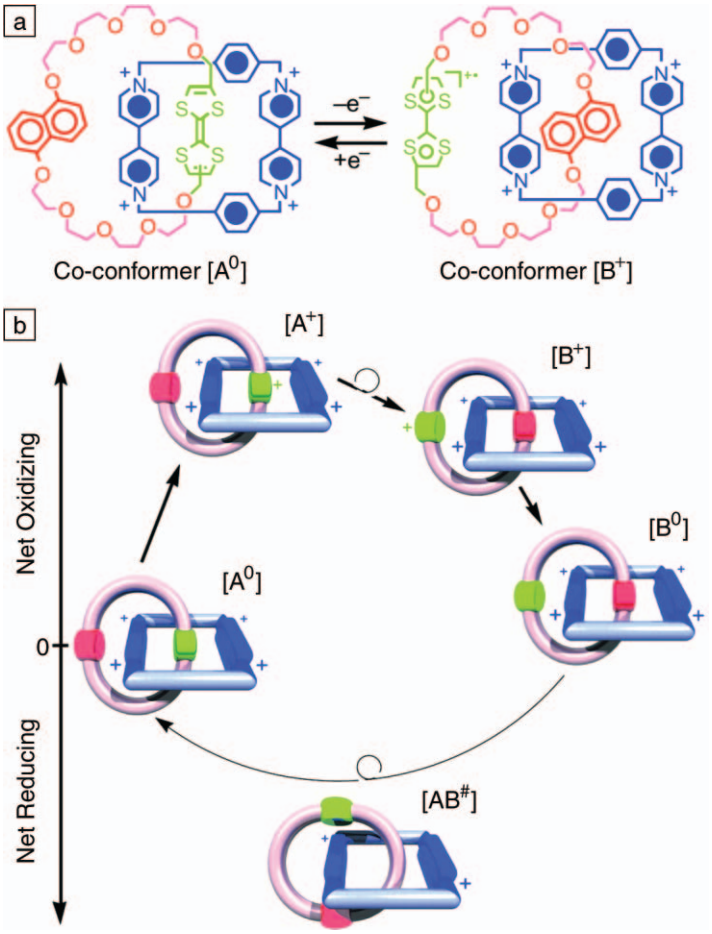

Figure 1. (a) Structure of the bistable catenane used in Reference 22. The voltage-driven circumrotation of co-conformer [A^0] to co-conformer [B^+] is the basis of the device. (b) Proposed mechanochemical mechanism for the operation of the device. Co-conformer [A^0] represents both the ground-state structure of the catenane and the "open switch" state of the device. When the catenane is oxidized (by applying a bias of −2 V), the tetrathiafulvalene groups (green) are ionized and experience a Coulomb repulsion with the tetracationic cyclophane (blue), resulting in the circumrotation of the ring and the formation of co-conformer [B^+]. When the voltage is reduced to a near-zero bias, the co-conformer [B^0] is formed, and this represents the "closed switch" state of the device.

A high-density molecular memory using a similar bistable molecule was demonstrated by Chen et al.[24] The two metal electrodes have a width of only 40 nm, and were made using imprint lithography. They reported an ON/OFF ratio of 10^3 to 10^4.

Another molecular memory uses molecules with functional groups. Reed et al. reported electrical bistability observed on a self-assembled monolayer of phenylethylene oligomers functionalized with NH_2 and NO_2 groups.[25] The molecular device exhibits two voltage-driven conductivity states. Hence, ideally one molecule will correspond to one bit. Several mechanisms have been proposed to explain the switching between the two conductivity states.[26–29] Seminario et al. proposed that charging of the molecule and subsequent localization/delocalization of molecular orbitals is the mechanism; Cornil et al. found that bias-induced alignment of molecular orbitals is the reason; and Taylor et al. proposed that the functionalization of the molecule has a significant effect on the interaction within the monolayer.

OBD Device Structure and Typical Current–Voltage Characteristics

The previous section of this article described the great range of approaches that have been taken by various research groups to produce a memory device based on organic films. The rest of the article will focus on our research into the organic bistable device (OBD) and its application in thin-film

memory cells. Our organic bistable device consists of a three-layer structure (organic/metal nanoclusters/organic) sandwiched between an anode and a cathode, as shown in the schematic inset of Figure 2.[14–19] The organic material we used is 2-amino-4,5-imidazoledicarbonitrile (AIDCN), with aluminum for the middle metal layer and the two outer electrodes. A typical OBD is shown in the micrograph inset in Figure 2. Details on the device fabrication can be found elsewhere.[14–18]

OBDs work in a variety of environments, including vacuum, N_2, and air. Unless otherwise specified, all electrical tests reported here were conducted in ambient conditions without any device encapsulation. The graph in Figure 2 shows typical *I–V* curves for an OBD. The first voltage scan from 0 V to 5 V, depicted by Curve A, shows a sharp increase in the current at about 2 V. After this transition, the device remains in this state, even after the power is turned off. This can be seen in Curve B, the second voltage scan. Curve C shows the *I–V* characteristics of the device after the application of a bias of –3 V, indicating the rewritability of the OBD.

Formation of the Metal Nanocluster Layer of the OBD

In our earlier studies of OBDs,[14–15] the middle Al nanocluster layer was formed by evaporating aluminum at a low deposition rate (0.5 Å/s) in a vacuum of 10^{-6} torr. Under such a slow evaporation rate and a background of oxygen, the evaporated Al vapor formed Al nanoclusters (consisting of metallic Al cores with oxide coatings) that were deep blue in color, rather than a shiny metallic color. To achieve more controllable device fabrication conditions, we developed a method for metal nanocluster formation by purposely providing a small amount of AIDCN vapor during Al evaporation. By carefully adjusting the Al:AIDCN volume ratio, we found that the optimum ratio of Al:AIDCN for the formation of the Al nanocluster layer in our chamber was ~3:1–4:1, where the device yield is over 95% percent. It should be noted that a variation in the Al:AIDCN ratio is possible if different evaporators are used. Under these fabrication conditions, the mixed film shows well-controlled nanocluster morph-ology, as shown in the atomic force microscope image in Figure 3 of the surface of an Al:AIDCN layer (volume ratio of Al:AIDCN = 3.3:1).

Polarization of the Metal Nanocluster Layer and Charge Storage Mechanism

The middle Al layer of an OBD consists of stacked nanoclusters, each consisting of a

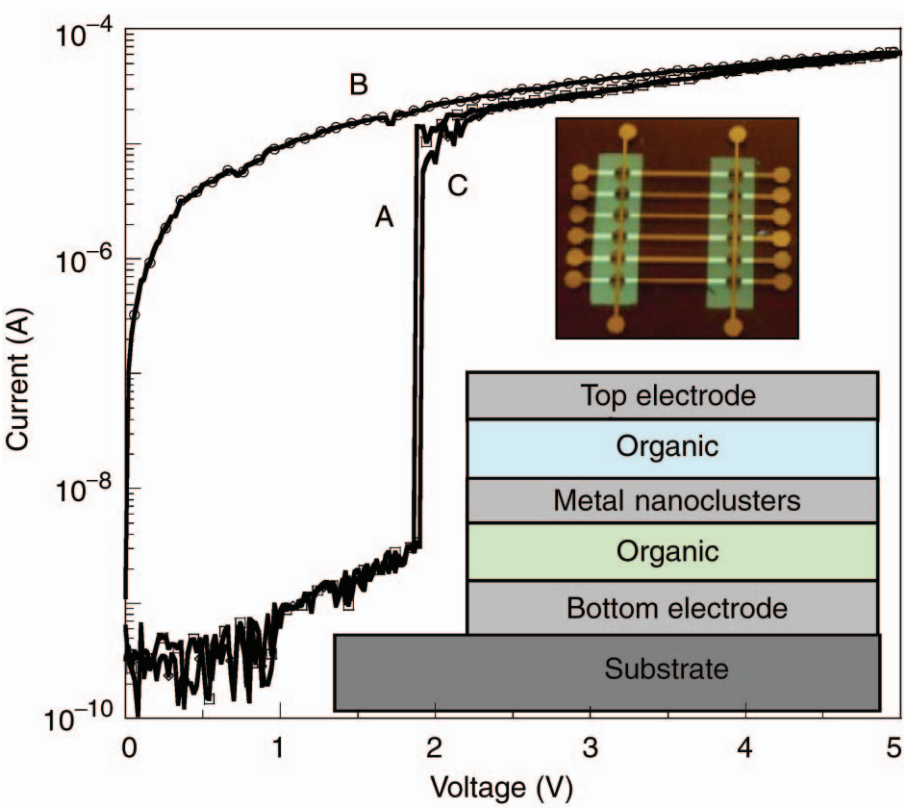

Figure 2. Typical current–voltage (I–V) characteristics of an organic electrical bistable device (OBD) with the nominal structure Al/AIDCN(50 nm)/Al(20 nm)/AIDCN(50 nm)/Al (AIDCN is 2-amino-4,5-imidazoledicarbonitrile). Curves marked A and B represent the I–V characteristics of the first and second bias scan, respectively. Curve C is the I–V curve of the third bias scan after the application of a reverse voltage pulse (−3 V). The lower inset shows a schematic of the device structure, and the upper inset is a micrograph of a typical OBD. The electrodes are 0.5 mm wide.

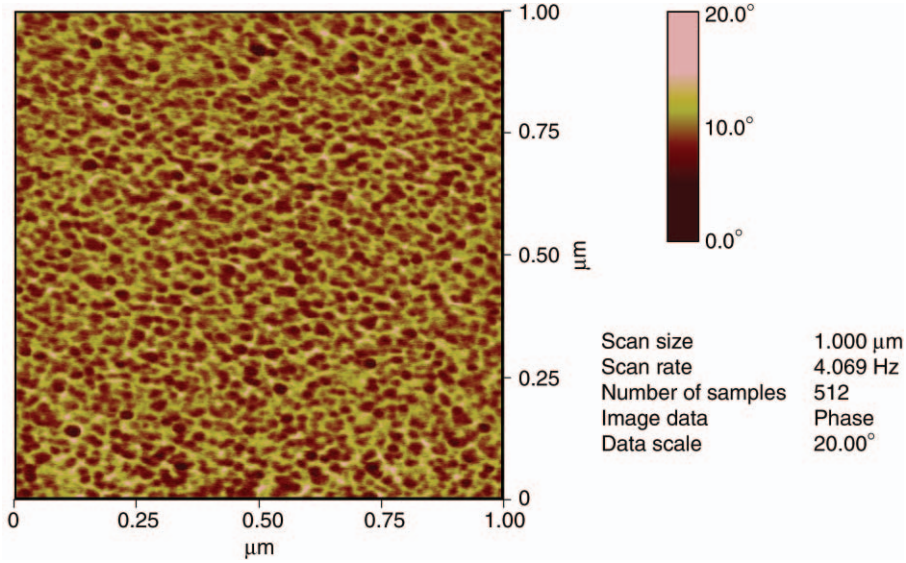

Figure 3. An atomic force microscope phase image of the surface of an Al:AIDCN layer (volume ratio Al:AIDCN = 3.3:1), indicating that the middle layer of the organic bistable device has a metalorganic nanocomposite structure. Pure metallic films in the middle layer result in device failure, so the metal nanoclusters formed in this method are important to the memory operation.

metallic core and an Al oxide shell (resulting from the reaction of Al with AlDCN or/and oxygen during the coevaporation process), with a very thin oxide layer between them. The energy diagram of an unbiased Al nanocluster layer shows a distribution of many energy wells next to each other, sandwiched between the two organic layers with relatively high LUMO–HOMO (lowest unoccupied molecular orbital–highest occupied molecular orbital) energy levels.[18–19] When a sufficiently high bias is applied to the device, the middle metal nanocluster layer is polarized, which results in charge storage near the two metal/organic interfaces between the middle metal layer and the organic layers. This stored charge lowers the interfacial resistance and leads to the switching behavior. When the electrical bias is removed, the charge remains within the metallic cores of the nanoclusters because of the barrier provided by the insulating coatings, which causes the nonvolatile memory effect.

We have proposed a theoretical model considering the interaction among the electrode, the organic molecules, and the metal nanoclusters. The interaction between the organic molecules and the metal nanoclusters is considered by using the single-band Hubbard Hamiltonian and the electron transmission probability through the device. These were calculated for two cases.[19] In the first case, there is no charge storage in the metal nanoclusters (Figure 4a), while in the second case, positive and negative charges are stored on opposite sides of the nanocluster layer (inset of Figure 4b). It was found that the electron transmission probability increases by several orders of magnitude when the metal nanocluster layer is charged,[13,14] which basically explains the OBD behavior.

Device Switching Process, Write–Erase Cycle Tests, and Retention Capability

The switching time for an OBD is very fast, less than 20 ns (see inset in Figure 5).[16] This is shorter than the electron traveling time from the electrode to the middle layer, which is about 1 μs based on an AlDCN layer with a thickness of 50 nm and a charge mobility of 10^{-5} cm^2/V s. This fast switching time indicates that the switching is not caused by the charge injection and trapping process.

The switching voltage of an OBD, which is independent of temperature (Figure 5),[17] suggests a tunneling process as the switching mechanism rather than a thermal process, since charge injection, transportation, and trapping have a strong dependence on temperature.

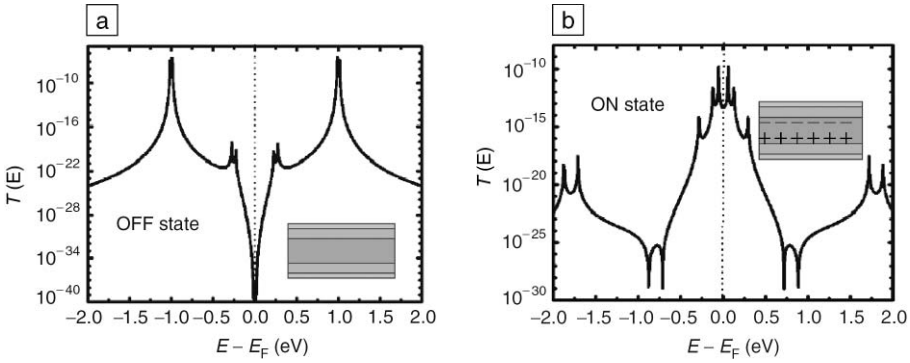

Figure 4. The transmission probabilities T(E) *as a function of energy for the following cases: (a) without charge in the nanocluster layer and (b) with positive and negative charges stored on opposite sides of the nanocluster layer. The insets show the corresponding device states.* E_F *is the Fermi level.*

More than 1 million write/erase cycles have been conducted on our OBDs with good rewritable characteristics, as shown in Figure 6. In addition to the rewriting capability, the memory retention of the ON and OFF states and the device performance under stress are important for practical applications. The memory retention ability was tested by leaving several OBDs in the ON state at ambient conditions. It was found that the devices remained in the ON state for several days to several weeks, indicating good memory retention characteristics relative to organic memories. However, for real applications, the retention time of memory cell should be in years, so more effort is necessary to improve this device for practical operations.

Summary

The device structure, fabrication, and characteristics of recently developed organic electrical bistable devices have been reviewed in this article. These devices have

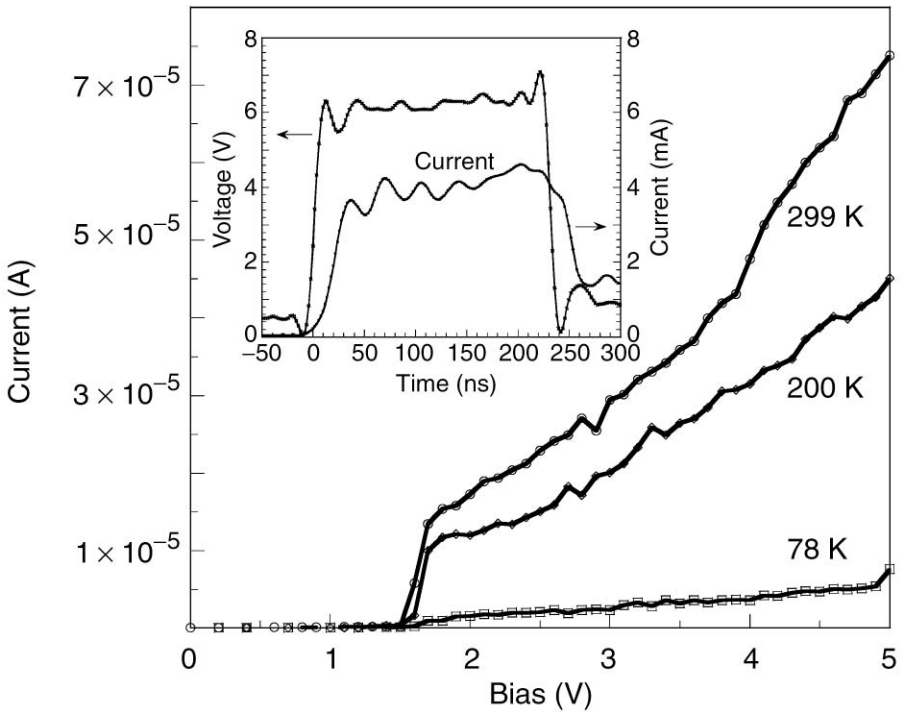

Figure 5. The switching I–V *curves of an organic bistable device (OBD) at various temperatures, showing that switching is independent of temperature. The inset shows the dynamic response of an OBD, initially in the OFF state, to an applied voltage pulse.*

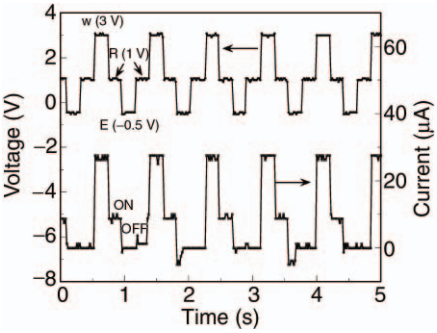

Figure 6. Typical current responses of an organic bistable device during write–read/erase–read voltage cycles. W stands for write, R for read. The upper trace is applied voltage; the lower trace is the device response.

strong potential as high-density, inexpensive nonvolatile electronic data storage for use in many applications such as electrically addressable random-access memory, flash memory, and electronic paper. The organic electrical bistable device (OBD) described here has a three-layer structure (organic/metal nanoclusters/organic) as the active medium, sandwiched between two electrodes. When a critical voltage pulse is applied to the device, polarization of the metal nanocluster layer leads to positive and negative charges stored on opposite sides of the nanocluster layer, which enhances the electron transmission probability of the device tremendously and turns the device to the ON state. These organic bistable devices open a new direction for organic electronics and will have a strong impact on our daily lives.

Acknowledgments

The authors gratefully acknowledge Dr. Jun He, Dr. Haiming Liem, Dr. Qianfei Xu, Mr. Chih-wei Chu, and Mr. Douglas Sievers for their contributions to the research discussed in this article. This research was partially supported by the U.S. Air Force Office of Scientific Research (F49620-03-1-0101, Dr. Charles Lee) and the National Science Foundation (DMR-0305111, Dr. LaVerne Hess).

References

1. J. Campbell Scott, *Science* **304** (2004) p. 62.
2. L.P. Ma, W.J. Yang, S.S. Xie, and S.J. Pang, *Appl. Phys. Lett.* **73** (1998) p. 3303; M.I. Lutwyche, M. Despont, U. Drechsler, U. Dürig, W. Häberle, H. Rothuizen, R. Stutz, R. Widmer, G.K. Binnig, and P. Vettiger, *Appl. Phys. Lett.* **77** (2000) p. 3299.
3. Li-Jie, E. Schreck, and K. Dransfeld, *Appl. Phys. A* **53** (1991) p. 457.
4. R.S. Potember and T.O. Poehler, *Appl. Phys. Lett.* **34** (1979) p. 407.
5. H. Carchano, R. Lacoste, and Y. Segui, *Appl. Phys. Lett.* **19** (1971) p. 414.
6. H.K. Henish and W.R. Smith, *Appl. Phys. Lett.* **24** (1974) p. 589.
7. Y. Segui, Bui Ai, and H. Carchano, *J. Appl. Phys.* **47** (1976) p. 140.
8. H. Carchano, R. Lacoste, and Y. Segui, *Appl. Phys. Lett.* **19** (1979) p. 414.
9. T. Oyamada, H. Tanaka, K. Matsushige, H. Sasabe, and C. Adachi, *Appl. Phys. Lett.* **83** (2003) p. 1252.
10. A. Bandyopadhyay and A.J. Pal, *Appl. Phys. Lett.* **82** (2003) p. 1215.
11. S. Moller, C. Perlov, W. Jackson, C. Taussig, and S.R. Forrest, *Nature* **426** (2003) p. 166.
12. S. Moller, S.R. Forrest, C. Perlov, W. Jackson, and C. Taussig, *J. Appl. Phys.* **94** (2003) p. 7811.
13. L.P. Ma, Q.F. Xu, and Y. Yang, *Appl. Phys. Lett.* **84** (2004) p. 4908.
14. Y. Yang, L.P. Ma, and J. Liu, U.S. Patent Pending, US 01/17206 (2001).
15. L.P. Ma, J. Liu, S.M. Pyo, and Y. Yang, *Appl. Phys. Lett.* **80** (2002) p. 362.
16. L.P. Ma, J. Liu, and Y. Yang, *Appl. Phys. Lett.* **80** (2002) p. 2997.
17. L.P. Ma, J. Liu, S.M. Pyo, Q.F. Xu, and Y. Yang, *Mol. Cryst. Liq. Cryst.* **378** (2002) p. 185.
18. L.P. Ma, S.M. Pyo, Q.F. Xu, and Y. Yang, *Appl. Phys. Lett.* **82** (2003) p. 1419.
19. J. Hubbard, *Proc. R. Soc. London, Ser. A* **276** (1963) p. 238; J.H. Wu, L.P. Ma, and Y. Yang, *Phys. Rev. B* **69** (2004) p. 11531.
20. L.D. Bozano, B.W. Kean, V.R. Deline, J.R. Salem, and J.C. Scott, *Appl. Phys. Lett.* **26** (2004) p. 607.
21. G. Jabbour, private communication.
22. C.P. Collier, G. Mattersteig, E.W. Wong, Y. Luo, K. Beverly, J. Sampaio, F.M. Raymo, J.F. Stoddart, and J.R. Heath, *Science* **289** (2000) p. 1172.
23. A.R. Pease, J.O. Jeppesen, J.F. Stoddart, Y. Luo, C.P. Collier, and J.R. Heath, *Acc. Chem. Res.* **34** (2001) p. 433.
24. Y. Chen, D.A.A. Ohlberg, X. Li, D.R. Stewart, R.S. Williams, J.O. Jeppesen, K.A. Nielsen, J.F. Stoddart, D.L. Olynick, and E. Anderson, *Appl. Phys. Lett.* **82** (2003) p. 1610.
25. M.A. Reed, J. Chen, A.M. Rawlett, D.W. Price, and J.M. Tour, *Appl. Phys. Lett.* **78** (2001) p. 3735.
26. J.M. Seminario, A.G. Zacarias, and J.M. Tour, *J. Am. Chem. Soc.* **122** (2000) p. 3015.
27. J.M. Seminario, A.G. Zacarias, and P.A. Derosa, *J. Phys. Chem. A* **105** (2001) p. 791.
28. J. Cornil, Y. Karzazi, and J.L. Bredas, *J. Am. Chem. Soc.* **124** (2002) p. 3516.
29. J. Taylor, M. Brandbyge, and K. Stokbro, *Phys. Rev. B* **68** 121101 (2003). □